

Decadal climate variability of the North Sea during the last millennium reconstructed from bivalve shells (*Arctica islandica*)

The Holocene
2014, Vol. 24(7) 771–786
© The Author(s) 2014
Reprints and permissions:
sagepub.co.uk/journalsPermissions.nav
DOI: 10.1177/0959683614530438
hol.sagepub.com


Hilmar A Holland, Bernd R Schöne, Constanze Lipowsky and Jan Esper

Abstract

Uninterrupted, annually resolved paleoclimate records are crucial to contextualize the current global change. Such information is particularly relevant for the Europe realm for which weather and climate projections are still very challenging if not virtually impossible. This study presents the first precisely dated, annually resolved, multi-regional *Arctica islandica* chronologies from the North Sea which cover the time interval AD 1040–2010 and contain important information on supra-regional climatic conditions (sea surface temperature (SST), ocean productivity, wind stress). Shell growth varied periodically on timescales of 3–8, 12–16, 28–36, 50–80, and 120–240 years, possibly indicating a close association with the North Atlantic Oscillation, ocean-internal cycles of the North Atlantic controlled by ocean–atmosphere couplings, and the Atlantic Multi-Decadal Oscillation. Increased climatic instability, that is, stronger quasi-decadal variability, seems to be linked to the predominance of atmospheric forcings and some significantly decreased insolation phases (e.g. Spörer and Maunder Minima). Increased climatic variability of shorter timescales was also observed during some particularly warm phases or regime shifts (e.g. during the ‘Medieval Climate Anomaly’ and since c. 1970). More stable climatic conditions, that is, extended warm or cold periods (‘Medieval Climate Anomaly’, ‘Little Ice Age’), however, fell together with a predominance of multi-decadal oceanic cycles. Whether the sunspot number and the higher frequency climate variability are causally linked and which processes and mechanisms are required lie beyond this study.

Keywords

annual increment width, Atlantic Meridional Overturning Circulation, bivalve sclerochronology, dendrochronology, North Atlantic Oscillation, sunspot number, wavelet analysis

Received 24 June 2013; revised manuscript accepted 18 February 2014

Introduction

Uninterrupted, long-term, high-resolution paleoenvironmental proxy data provide an essential means to test and verify numerical climate models (IPCC, 2007; Jones et al., 2001, 2009) and contextualize present climate change. Such data are particularly relevant for Europe and adjacent marine settings for which weather and climate predictions beyond timescales of several days are virtually impossible at present (Woollings, 2010). The difficulty to predict future change in this region results from (1) the dynamic and non-stationary behavior of oceanic and atmospheric circulation patterns that govern European climate (Greatbatch, 2000), that is, the Atlantic Meridional Overturning Circulation (AMOC; Delworth and Mann, 2000; Schlesinger and Ramankutty, 1994; Wei et al., 2012) and the North Atlantic Oscillation (NAO; Hurrell, 1995; Van Loon and Rogers, 1978) and (2) the lack of sufficient long-term, high-resolution paleoclimate datasets.

Numerous terrestrial, annually resolved paleoclimate archives (e.g. tree rings – Briffa et al., 1992; Esper et al., 2002; Grudd et al., 2002; stalagmites – Fohlmeister et al., 2012; Scholz et al., 2012; Vollweiler et al., 2006; varved lake sediments – Sirocko et al., 2012) spanning centuries to millennia have yielded unique insights into the European climate history and highlighted potential links to cultural transformations (Büntgen et al., 2012). However, one major drawback of these records is that they tend to be

biased toward summer, whereas environmental variables during other seasons are only indirectly recorded. Furthermore, a more detailed understanding of the European climate also requires knowledge of environmental variability in adjacent oceans, specifically the North Sea, which exerts a direct influence on climate of the littoral states.

As demonstrated by several recent studies, shells of long-lived bivalve mollusks, in particular the ocean quahog, *Arctica islandica*, contain detailed records of decadal to century-scale environmental change in the northern North Atlantic (Schöne et al., 2003; Wanamaker et al., 2012; Witbaard et al., 1997). Based on synchronous changes in shell growth and a common response to environmental fluctuations, increment width time-series of specimens with overlapping life spans can be combined by means of cross-dating (wiggle-matching) into single composite or master

University of Mainz, Germany

Corresponding author:

Bernd R Schöne, Institute of Geosciences, University of Mainz, Joh.-J.-Becher-Weg 21, 55128 Mainz, Germany.
Email: schoeneb@uni-mainz.de

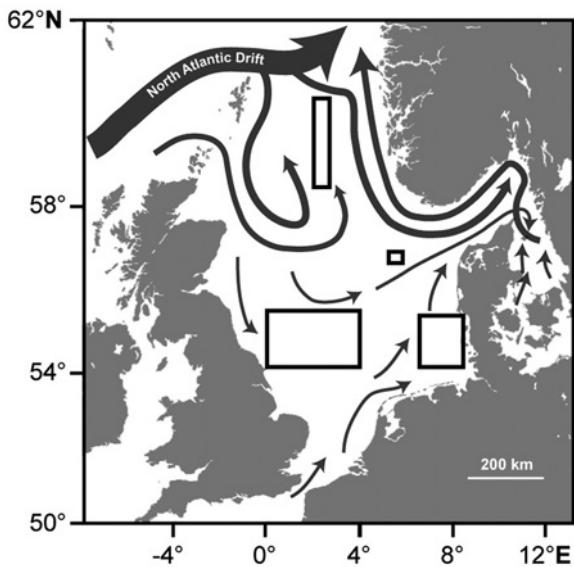


Figure 1. Map showing sampling regions of *Arctica islandica* in the North Sea and major currents. Map based on Turrell (1992) and Turrell et al. (1992). Not included are the Fladen Ground specimens of the study by Scourse et al. (2006). Shells are divided into three groups: Norwegian Sea (upper box), Doggerbank (left box), and Eastern North Sea (right boxes). For a detailed list of samples, see Table 1.

chronologies (Butler et al., 2010; Marchitto et al., 2000; Schöne et al., 2003; Thompson et al., 1980; Witbaard et al., 1997). This time-series can cover centuries to millennia, including many generations of bivalves and provide information on common environmental variables that influenced the growth of all studied specimens. Furthermore, these chronologies serve as a framework to place geochemical proxy data, for example, stable oxygen and carbon isotope values or trace element data of the shells into a precise temporal context (Schöne et al., 2005b, 2011; Wanamaker et al., 2012).

Here, we present the first millennial-scale *A. islandica* chronologies from the North Sea. Our study mainly addresses the following questions: Which quasi-decadal and multi-decadal variability is recorded by the shells? Is the relative strength of these oscillations changing through time and why? Which environmental variables are recorded by the shells? Results of our study can be used to better understand the climate history in the northeast Atlantic realm and help to better constrain numerical climate models.

Material and methods

A total of 51 shells of *A. islandica* were obtained from several localities of the North Sea by means of bottom trawling and ring-dredge fishing (Figure 1, Table 1). All studied specimens lived below the thermocline between *c.* 20 and 115 m water depth. In all, 31 specimens were well-preserved fossils without external signs of erosion or diagenesis. Even the periostracum, which is prone to quick decay after death, was well preserved. The remaining individuals were collected alive. Three additional time-series taken from the floating chronology of Scourse et al. (2006) were combined with our chronologies in order to increase the sample depth (number of specimens per time interval).

Radiocarbon dating

In order to place the fossil shells in a temporal context, 16 specimens were dated by means of $^{14}\text{C}_{\text{AMS}}$ (Table 1). For this purpose, 70–100 mg of carbonate powder was milled from the umbonal

shell portions covering *c.* 6 years of growth. Samples were analyzed by the Poznań Radiocarbon Laboratory, Poland. Radiocarbon dates (Libby years) were subsequently calibrated with the software tool CALIB 5.0.2 (<http://calib.qub.ac.uk/calib/>), assuming published marine reservoir correction (ΔR) values of 20 ± 42 and 14 ± 55 years (Harkness, 1983; Mangerud and Gulliksen, 1975), respectively. Datasets for the calibration are based on Stuiver et al. (1998) and Hughen et al. (2004).

Shell preparation and sclerochronological measurements

In preparation for shell growth pattern analysis, clean shells were mounted on Plexiglas cubes with a plastic welder (GlueTec Multipower). To avoid fractures during the sawing, a fast drying, two-component metal epoxy resin (WIKO Flüssigmetall) was applied along the axis of maximum growth. Along this axis, a 3-mm-thick section was cut from each specimen using a Buehler Isomet[®] 1000 low-speed precision saw equipped with a 0.4-mm-thick diamond-coated wafering saw blade. Shell slabs were mounted on glass slides and subsequently ground with 800 and 1200 SiC grit power and polished with $1 \mu\text{m}$ Al_2O_3 powder. Between each preparation step, samples were ultrasonically rinsed. To facilitate growth pattern analysis, the polished slabs were immersed in Mutvei's solution (Schöne et al., 2005a; Figure 2), which differentially etched the shell carbonate, stained sugars, and sugar precursors and preserved the organic matrices in three dimensions. Shell cross-sections were digitized with a Nikon Coolpix[®] 995 camera attached to a binocular microscope with sectoral dark field illumination (Schott VisiLED MC 1000). Annual increment widths were measured in the outer shell layer of the ventral margin and the hinge plate (Figure 2) with the image processing software Panopea (©Schöne & Peinl). The hinge record was used to verify the ventral margin record and to minimize potential measurement errors.

Cross-dating and temporal alignment of the sclerochronologies

The precise calendar alignment of the increment width chronologies (Figure 3) was accomplished by three different cross-dating methods: (1) visual cross-dating applying wiggle-matching and identifying pointer years (Schweingruber et al., 1990), (2) the dendrochronology software COFECHA (Grissino-Mayer, 2001), and (3) the JAVA[™]-based Shell-Aligner[©] software (programmed by one of us, CL). The fundamental difference between the two computer-aided alignment methods is that COFECHA focuses almost exclusively on the year-to-year agreement (higher frequency domain; correlation coefficients), whereas Shell-Aligner cross-dates chronologies based on the best agreement in the high- and low-frequency realm after removal of ontogenetic age trends by means of regional curve standardization (RCS). Shell-Aligner uses algorithms developed for the comparison of amino-acid sequences in molecular cell biology (Needleman and Wunsch, 1970; Smith and Waterman, 1981). Whereas Shell-Aligner requires age-detrended growth increment width chronologies; COFECHA processes raw chronologies. COFECHA applies a high-pass filter (here, a flexible cubic spline adjusted with a rigidity of 32 years and 50% frequency response in accordance with Butler et al., 2013) to each of the raw increment width chronologies, computes normalized growth indices (ratios of measured divided by predicted growth values), removes the autocorrelation from the time-series, and provides suggestions for the temporal alignment of the data (least squares method) by indicating how the agreement could be increased by adding or deleting growth increments.

Based on these cross-dating techniques, annual increment width time-series of live-collected and fossil shells with overlapping life

Table 1. List of specimens of *Arctica islandica* used in this study including radiometric ages of fossil shells.

Group	Sample ID	Locality	Water depth	Ontogenetic age	Collected dead (D)/ alive (A) in yr AD	¹⁴ C _{AMS} yr BP	2σ cal. yr AD
Norwegian Sea	WH241-603-BoxL-D1R	58°47.80'N, 2°39.43'E	116	109	(D) 2002	1190 ± 30	1070–1330
	WH241-604-BoxL-D8L	58°43.68'N, 2°39.35'E	113	81	(D) 2002	1110 ± 30	1180–1420
	WH241-604-BoxL-D13R	58°43.68'N, 2°39.35'E	113	81	(D) 2002	535 ± 25	1691–recent
	WH241-611-BoxL-D1L	58°28.81'N, 2°18.29'E	113	151	(D) 2002	580 ± 25	1647–recent
	WH241-611-BoxL-D2R	58°28.81'N, 2°18.29'E	113	141	(D) 2002	605 ± 25	1570–1900
	WH241-611-BoxL-D3L	58°28.81'N, 2°18.29'E	113	103	(D) 2002	525 ± 25	1696–recent
	WH241-612-BoxL-D3R	58°48.87'N, 2°29.27'E	113	74	(D) 2002	550 ± 25	1670–recent
	WH241-615-BoxL-D5R	58°41.54'N, 2°37.57'E	110	152	(D) 2002	580 ± 40	1652–recent
	WH241-615-BoxL-D6R	58°41.54'N, 2°37.57'E	110	91	(D) 2002	1155 ± 30	1120–1390
	WH241-617-BoxL-D6L	58°45.22'N, 2°35.46'E	112	189	(D) 2002	890 ± 40	1325–1588
	WH241-621-BoxM-D10R	60°21.33'N, 2°30.03'E	94	64	(D) 2002	120 ± 40	Recent
	WH241-635-BoxM-D2L	60°19.09'N, 2°28.19'E	100	120	(D) 2002	470 ± 30	1719–recent
	WH241-637-BoxM-D10L	60°22.06'N, 2°32.04'E	90	182	(D) 2002	665 ± 25	1510–1820
	WH254-BoxM-D9R	60°21.91'N, 2°32.07'E	86–145	82	(D) 2002	60 ± 40	Recent
	WH254-46F2-Box L-A1R	58°45.06'N, 2°29.78'E	>90	76	(A) 2003		
	WH254-599-Box L-A1R	58°42.30'N, 2°25.28'E	105	17	(A) 2002		
	WH254-599-Box L-A2R	58°42.30'N, 2°25.28'E	105	30	(A) 2002		
	WH254-Box M-A1R	60°21.91'N, 2°32.07'E	86–154	32	(A) 2002		
	WH254-Box M-A2L	60°21.91'N, 2°32.07'E	86–145	35	(A) 2002		
	WH254-Box M-A4R	60°21.91'N, 2°32.07'E	86–145	72	(A) 2002		
	WH254-Box M-A5L	60°21.91'N, 2°32.07'E	86–145	30	(A) 2002		
	WH254-Box M-A6R	60°21.91'N, 2°32.07'E	86–145	68	(A) 2002		
	WH254-Box M-A102L	60°21.91'N, 2°32.07'E	86–145	29	(A) 2002		
05-III-ST13-A1R	58°36.75'N, 2°20.50'E	104–105	51	(A) 1905			
Doggerbank	WH241-677-BoxB-D3L	55°23.91'N, 0°1.84'W	79	85	(D) 2002	630 ± 40	1528–1885
	2011-WH-DOGT-7-KU-D1R	54°48.91'N, 1°26.22'E	66–70	124	(D) 2011		
	2011-WH-DOGT-T1-KU-D7L	54°09.90'N, 1°19.13'E	67–70	98	(D) 2011		
	2011-WH-DOGT-T1-KU-D8L	54°09.90'N, 1°19.13'E	67–70	46	(D) 2011		
	2011-WH-DOGT-T1-KU-A9L	54°09.90'N, 1°19.13'E	67–70	15	(A) 2011		
	2011-WH-DOGT-T4KU-D10R	55°34.21'N, 2°20.10'E	64–69	74	(D) 2011		
	2011-WH-DOGT-T4KU-A11L	55°34.21'N, 2°20.10'E	64–69	100	(A) 2011		
	2011-DOGU-5-RD-D1L	54°37.28'N, 1°41.59'E	24	134	(D) 2011		
	2011-DOGU-11-KU-D2R	54°44.81'N, 2°01.02'E	34–35	76	(D) 2011		
	2011-DOGT-22-KU-D1L	54°46.83'N, 2°33.06'E	21	115	(D) 2011		
	DOG-K9-KU-D1L	54°59.70'N, 1°40.00'E	26–30	115	(D) 2003		
	DOG-K9-KU-D2L	54°59.70'N, 1°40.00'E	26–30	61	(D) 2003		
	DOG-K10-KU-D2L	54°54.70'E, 1°47.53'E	26–28	102	(D) 2003		
	DOG-K11-KU-D1L	54°45.06'N, 2°0.93'E	32–34	57	(D) 2003		
	DOG-K29-KU-D1L	55°08.01'N, 2°41.05'E	27–28	97	(D) 2003		
	DOG-K36-KU-D1L	55°18.87'N, 3°18.57'E	29	172	(D) 2003		
	DOG-K39-KU-D1L	55°28.71'N, 3°59.25'E	31–32	102	(D) 2003		
Eastern North Sea	WH241-572-RA6-A1R	54°45.83'N, 7°16.37'E	27	112	(A) 2002		
	WH254-560-40F7-A1L	55°45.06'N, 7°29.81'E	23	125	(A) 2003		
	WH254-596-Box C-A1R	56°45.06'N, 5°29.80'E	~60	41	(A) 2002		
	M071868-A1L	53°55.27'N, 8°30'E	30	74	(A) 1848		
	M071868-A10L	54°10'N 7°53'E	30	108	(A) 1868		
	M071868-A11R	54°10'N 7°53'E	30	93	(A) 1868		
	SM308688-D1R	55°13'N, 6°34'E	39	49	(A) 1977		
	SM308688-D2L	55°13'N, 6°34'E	39	65	(A) 1977		
	AV04-14-VC-D1R	~54°10'N 7°53'E	<30 m; core: 70 cm	36	(D) 2005	<775 ± 35	>1610–1730
	AV04-15-VC-D3L	~54°10'N 7°53'E	<30 m; core: 235 cm	141	(D) 2005	775 ± 35	1610–1730
Scourse et al. (2006)	010088	58°49.86'N, 0°21.35'W	115	117	(D) 2001	1138 ± 36	1242–1297 (1σ)
	010090	58°49.86'N, 0°21.35'W	115	227	(D) 2002	1309 ± 38	1044–1154 (1σ)
	010099	58°49.86'N, 0°21.35'W	115	267	(D) 2003	1266 ± 38	1076–1195 (1σ)

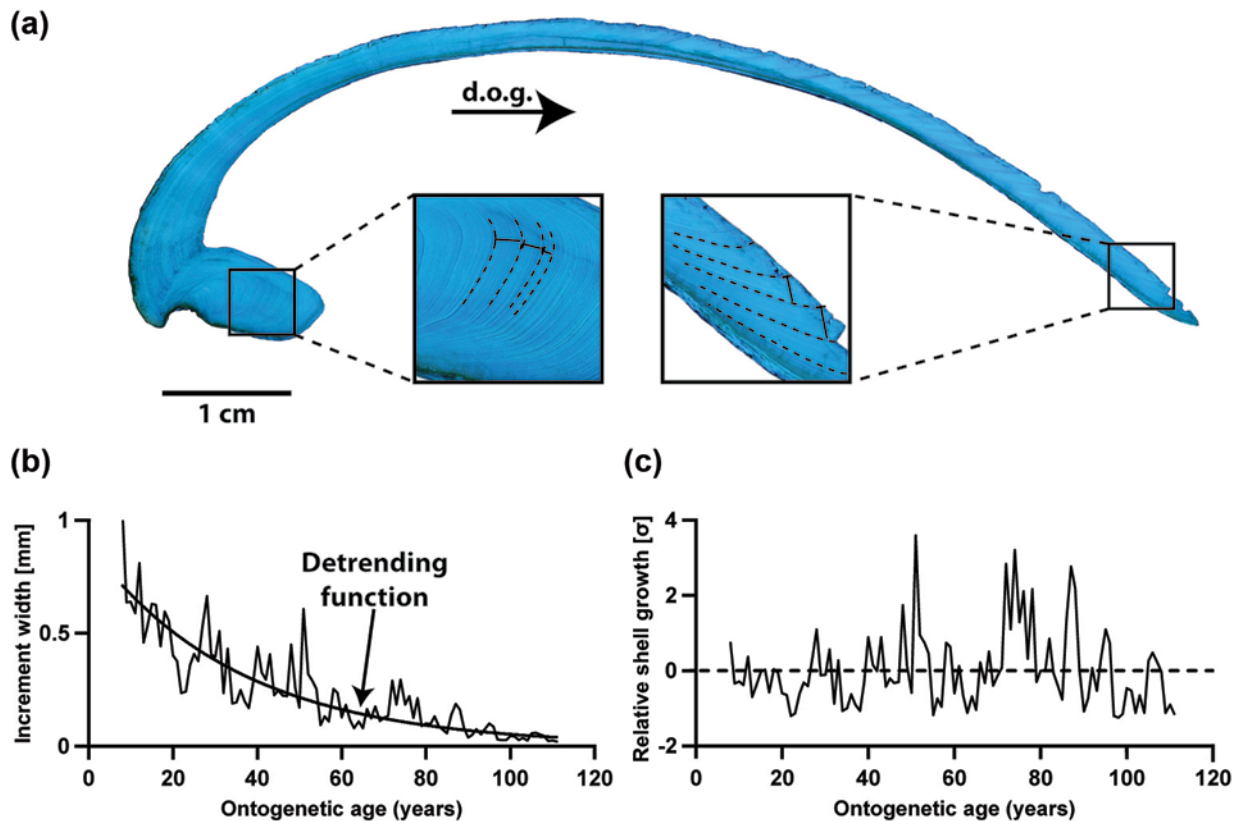


Figure 2. Sclerochronological analysis of *Arctica islandica* shells. (a) Cross-section immersed in Mutvei's solution showing distinct annual growth lines and increments in the outer shell layer of the hinge portion (left) and the ventral margin (right). (b) Annual increment widths and the variance decrease through ontogeny. The trend toward narrower increments at later stages of life can be estimated with a growth function ('detrending function') and mathematically eliminated from the time-series. (c) After detrending and standardization, relative changes in shell growth can be studied. d.o.g.: direction of growth.

spans were precisely temporally aligned. Radiocarbon dates facilitated the cross-dating of fossil shells by placing them in a narrow temporal window of the past. Some fossil shells, however, did not overlap with modern shells or precisely chronologically aligned fossil shells. To assign absolute calendar dates to these shells, the chronologies were cross-dated with Scandinavian dendrochronologies (Esper et al., 2012; Grudd et al., 2002). This method has previously been used by Schöne and Fiebig (2009) and is based on the notion that bivalves from the North Sea and trees from northern Scandinavia share common signals. The presence of common environmental forcings on bivalves and trees has also been demonstrated by Black et al. (2009) and Black (2009) in the US NW Pacific.

Age-detrending and chronology construction

To isolate environmental signals, ontogenetic age trends (decreasing growth rates and decreasing year-to-year variance with increasing age) were removed from the shell chronologies by the following statistical methods (Figure 2): (1) Negative exponential (NE_{ARSTAN}) detrending and standardization using the dendrochronology software ARSTAN (Cook, 1986). In addition to low-pass filtering (trend estimation), ARSTAN pre-whitened the time-series (removal of lag-1 autocorrelation) and performed a variance stabilization (removal of high correlation between the local mean and variance, production of homoscedastic time-series; Cook and Peters, 1997). (2) Regional curve detrending and RCS, a less flexible age trend-elimination method (Briffa et al., 1992). For RCS, a single ontogenetic growth curve was computed for the hinge and ventral margin records of all studied specimens and then applied to eliminate ontogenetic age trends of individual

shell chronologies. (1) A seventh-order polynomial fit was used to estimate the ontogenetic age trend of all studied specimens. Growth indices for each year were then computed by dividing measured by predicted growth. For the manually constructed RCS chronology (RCS_{manual}), GI values at each year were arithmetically averaged. For comparison with other chronologies, the resulting time-series was mathematically standardized by subtracting the mean and dividing by the standard deviation (SGI values). (2) In addition, ARSTAN was used for RCS, including pre-whitening of the shell growth data (RCS_{ARSTAN}). At each year, ARSTAN calculated a bi-weighted mean of the growth indices.

In order to strengthen the sample depth in older sections of the chronologies, three time-series of the Fladen Ground floating chronology by Scourse et al. (2006) were cross-dated and incorporated in further versions of the RCS_{manual} and the NE_{ARSTAN} series, respectively. Based on methodological differences, our RCS_{manual} detrending procedure was inapplicable to the Fladen Ground time-series. The latter were detrended by a relatively rigid, 75-year cubic smoothing spline that also preserves parts of the low-frequency domain.

To evaluate the agreement of shell growth dynamics among the different sampling areas, three local time-series were calculated (Norwegian Sea, RCS_{NORS} ; Doggerbank, RCS_{Dogger} ; Eastern North Sea, RCS_{ENS}). Together with the standardized mean Fladen Ground record of Scourse et al. (2006), they were then used to compile an average composite chronology (composite RCS_{manual}), where each locality takes equal account. Given the low number of local time-series and the variable coverage of time (including temporal gaps) of each time-series, a 'nested' approach as demonstrated in Cunningham et al. (2013) and Wilson et al. (2010) or a procedure as in Reynolds et al. (2013) was not carried out.

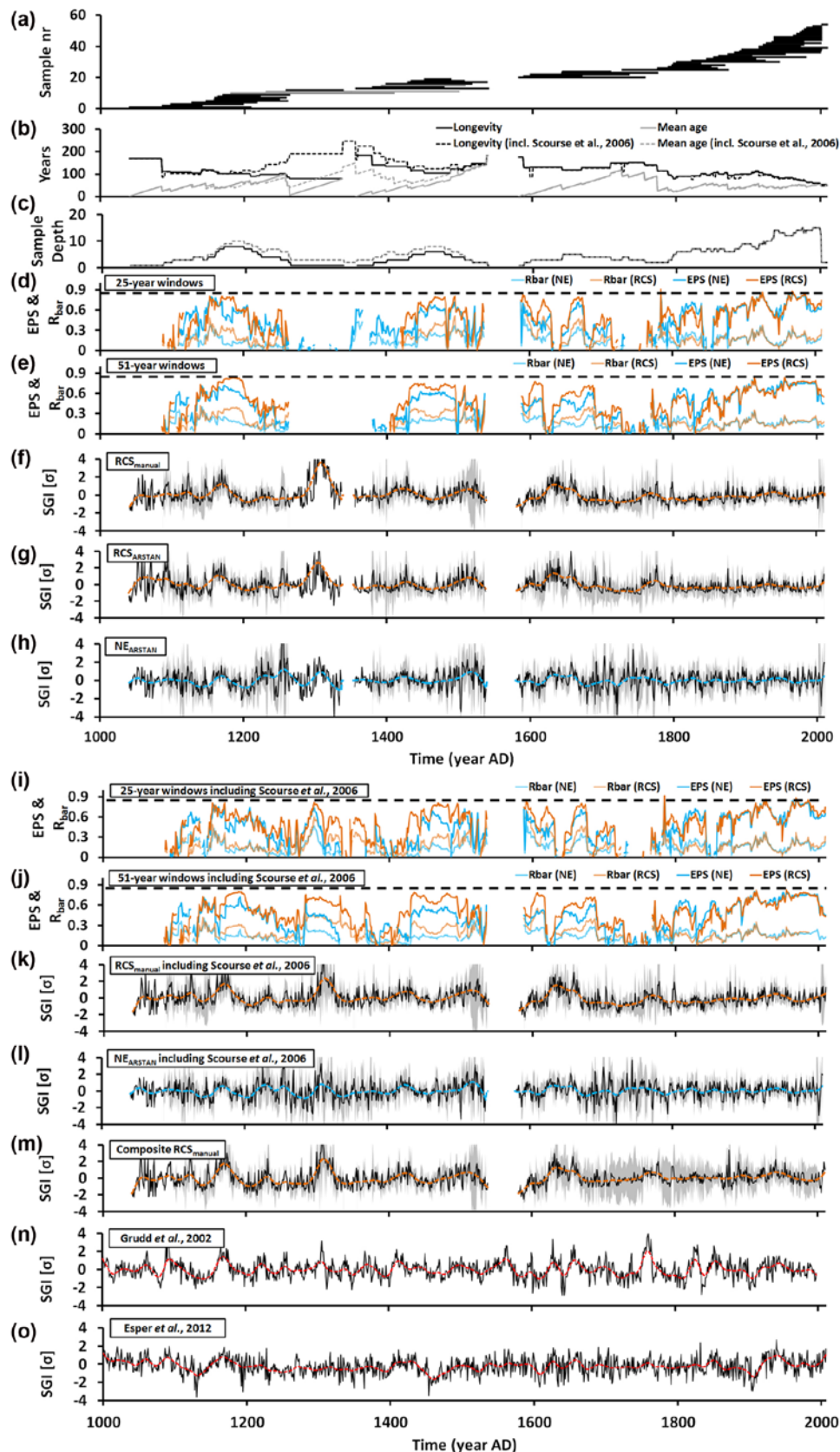


Figure 3. Multiregional *Arctica islandica* composite chronology from the North Sea and statistical measures. (a) Life spans of specimens. Each horizontal line corresponds to a single individual. Gray bars represent the three specimens used in the study by Scourse et al. (2006). (b) Longevity and mean age through time. (c) Sample depth = number of specimens per time interval. (d and e) Estimated population strength (EPS) and inter-series correlation coefficient (R_{bar}) in running 25- and 51-year windows. Dashed horizontal lines reflect the 0.85 threshold of Wigley et al. (1984). Standardized chronologies based on different detrending techniques: (f) $\text{RCS}_{\text{manual}}$, (g) $\text{RCS}_{\text{ARSTAN}}$, (h) $\text{NE}_{\text{ARSTAN}}$. Gray lines denote 95% confidence intervals. (i and j) Estimated population strength (EPS) of dataset, including the three time-series of Scourse et al. (2006) in 25- and 51-year windows. (k to m) Standardized chronologies based on different detrending techniques, including Scourse et al. (2006). (k) $\text{RCS}_{\text{manual}}$, (l) $\text{NE}_{\text{ARSTAN}}$, and (m) Composite chronology. (n and o) Scandinavian dendrochronologies (Esper et al., 2012; Grudd et al., 2002) shown for comparison with the bivalve sclerochronology. These tree-ring master chronologies were also used to cross-date floating chronologies and place $^{14}\text{C}_{\text{AMS}}$ dated fossil shells in a precise temporal context. Flexible cubic splines with a rigidity of 25 years f–h and k–o were computed to facilitate recognition of common low-frequency oscillations.

The robustness of the chronologies was evaluated by the expressed population signal (EPS) value (Briffa and Jones, 1990; Wigley et al., 1984).

$$\text{EPS} = \frac{n \cdot R_{\text{bar}}}{(n \cdot R_{\text{bar}} + (1 - R_{\text{bar}}))} \quad (1)$$

where R_{bar} is inter-series correlation between pairs of GI chronologies, and n is the number of specimens used to construct the stacked chronology. The EPS value quantifies how well the composite chronology resembles the infinitely replicated, perfect chronology (Briffa and Jones, 1990; Wigley et al., 1984). According to Wigley et al. (1984), EPS values greater than 0.85 indicate that the variance of a single SGI chronology sufficiently expresses the common variance of all SGI series. EPS values computed in running 25-year and 51-year windows were used to demonstrate how the agreement between the GI series changed through time.

Time-series analyses

To identify the temporal dynamics of the composite chronologies, continuous wavelet transforms (CWTs) were computed (parameter value = 6; Torrence and Compo, 1998; Figure 8) with MATLAB R2012b using the ion wavelet script, available online at <http://ion.researchsystems.com/>. In order to properly perform the spectral analyses, gaps in the shell chronology were filled with data of the Scandinavian tree-ring chronology (Esper et al., 2012; Grudd et al., 2002). A univariate red-noise autoregressive lag-1 (AR(1)) model was applied as a background spectrum to evaluate the 5% significance level, that is, the 95% confidence level of the CWT.

Spatial correlation maps (Figure 7) were computed between the different chronology versions (NE_{ARSTAN}, RCS_{manual}, RCS_{ARSTAN}, RCS_{NORS}, RCS_{Dogger}, RCS_{ENS}) and meteorological data using the Koninklijk Nederlands Meteorologisch Instituut (KNMI) explorer (Trouet and Van Oldenborgh, 2013; <http://climexp.knmi.nl/>; last checked: 15 January 2013). Instrumental datasets included (1) the NOAA Optimum Interpolation Sea Surface Temperature (OI-SST) Analysis dataset v. 2, hereafter referred to as Reynolds OI-SST (Reynolds, 1988; Reynolds and Smith, 1995; Smith and Reynolds, 1998); (2) SST of the Hadley Centre Sea Ice and SST dataset, HadISST (Rayner et al., 2003); (3) the European Reanalysis surface temperature dataset of the European Centre for Medium-Range Weather Forecasts, ERA-40 (S)ST (Uppala et al., 2005); (4) the ERA-40 sea surface pressure, ERA-40 SSP; and (5) zonal wind stress fields, ERA-40 zw. In addition, the NAO index (Hurrell, 1995) during February–September was compared with all chronology variants and the different seasonal averages of the environmental datasets listed above. Spatial regression analyses of the shell chronology variants (NE_{ARSTAN}, RCS_{manual}, RCS_{ARSTAN}) was only conducted for years containing at least four shells (=prior to 2002). Additionally to the spatial correlation attempts, simple regression analysis at monthly and seasonal resolution was performed between the *A. islandica* chronologies and the instrumental datasets (Figure 6).

Results

Cross-dated growth increment time-series of the studied specimens of *A. islandica* from different localities in the North Sea (Figure 1) cover the time interval of AD 1040–2010 (Figure 3; note that all calendar years in this article are AD). The multiregional chronologies comprise an uninterrupted, absolutely dated portion stretching from 1581 to 2010 (35 shells) and two floating chronologies (6 and 10 shells; Table 1; Figure 3). As seen from the regression analysis (Figure 4), all three regional sub-chronologies share common signals. Based on ¹⁴C_{AMS} ages of umbonal shell

portions and cross-dating with the Scandinavian dendrochronologies (Esper et al., 2012; Grudd et al., 2002; highly significant correlation between growth of bivalves and trees: $R = 0.63$, $p < 0.0001$, 1900–1997, RCS_{manual}–Grudd; Figure 5), it was possible to assign absolute calendar dates to these floating chronologies: 1040–1336 and 1355–1538 (Figure 3). Hence, the North Sea chronologies exhibit two small temporal gaps of 18 and 42 years between 1337 and 1354 and between 1539 and 1580, respectively (Figure 3, without Torneträsk dendrochronology). By incorporating the three floating time-series of Scourse et al. (2006), it was possible to fill up the temporal gap between 1335 and 1355. This resulted in an uninterrupted chronology that extended from modern times back to 1538 (Figure 3).

During the 20th century, running EPS values exceeded the 0.85 threshold (Wigley et al., 1984). Prior to that time, EPS values remained below this critical threshold but were largely above 0.6 (Figure 3). EPS values closer to the critical threshold value defined by Wigley et al. (1984), that is, above 0.75 are normally accompanied by larger sample depths. Sharp signal declines were often associated with lower specimen numbers. Through cross-dating with the time-series by Scourse et al. (2006), it was possible to place the two oldest floating chronologies in an absolute temporal context and close the gap between the two time-series. However, because of the low sample depth, the EPS value still remained below 0.85. As expected by strongly fluctuating sample depths and the two major temporal gaps, average EPS values did not reach Wigley's critical threshold value. The average EPS value of the NE_{ARSTAN} chronology (0.52, $R_{\text{bar}} = 0.17$, $n = 5.31$) returned a slightly lower value than the RCS time-series (0.56, $R_{\text{bar}} = 0.19$, $n = 5.33$). Versions that include the Scourse et al. (2006) time-series showed hardly any improvements concerning the population signal (RCS_{manual}: EPS = 0.57, $R_{\text{bar}} = 0.19$, $n = 5.83$; NE_{ARSTAN}: EPS = 0.53, $R_{\text{bar}} = 0.16$, $n = 5.87$). The regional chronologies exhibited lower EPS values (RCS_{NORS}: EPS = 0.42, $R_{\text{bar}} = 0.17$, $n = 3.66$; RCS_{Dogger}: EPS = 0.57, $R_{\text{bar}} = 0.29$, $n = 3.15$; RCS_{ENS}: EPS = 0.43, $R_{\text{bar}} = 0.19$, $n = 3.26$). Maximum 25-year-running R_{bar} /EPS values ranged between 0.69/0.86 (NE_{ARSTAN}) and 0.81/0.91 (RCS_{manual}, RCS_{ARSTAN}; Figure 3).

Through the last millennium, the mean longevity of the studied specimens fluctuated between 49 and 184 years (Figure 3). During the 'Little Ice Age' (LIA), the average life span of *A. islandica* was 32 years longer than during the 'Medieval Climate Anomaly' and the Modern Warmth (Figure 3). Specifically, since the early 20th century, the average life span declined from 113 to 49 years (Figure 3). The oldest specimen of this study reached an ontogenetic age of 184 years. One shell of the Scourse et al. (2006) time-series was slightly older (227 years).

Fossil shells were not equally distributed through time, but exhibited four time intervals of high abundance, that is, *c.* 1170–1200, 1450–1475, 1640–1670, and after *c.* 1800 and four intervals of remarkably low abundance, that is, before *c.* 1085, 1260–1340, 1540–1580, and 1760–1790 (Figure 3).

Spectral analysis

Continuous wavelet transformation of five variants (NE_{ARSTAN}, RCS_{manual}, RCS_{ARSTAN}, RCS_{manual} with Scourse, Composite RCS_{manual}) of the chronology revealed distinct spectral power at frequencies corresponding to periods of 3–8, 12–16, 28–36, 50–80, and 120–240 years (Figure 8). The RCS chronologies were dominated by low-frequency oscillations (*c.* >28 years), whereas the higher frequency components were better preserved in the NE_{ARSTAN} time-series (Figure 8). All three RCS chronologies showed statistically significant (95% confidence interval) and temporally coherent signals in the 120- to 210-year band throughout the last millennium (Figure 8a, b, and d). Whereas these cycles are less developed in RCS_{ARSTAN}, they are pronounced in the chronologies that include the time-series of Scourse et al. (2006); these modes also

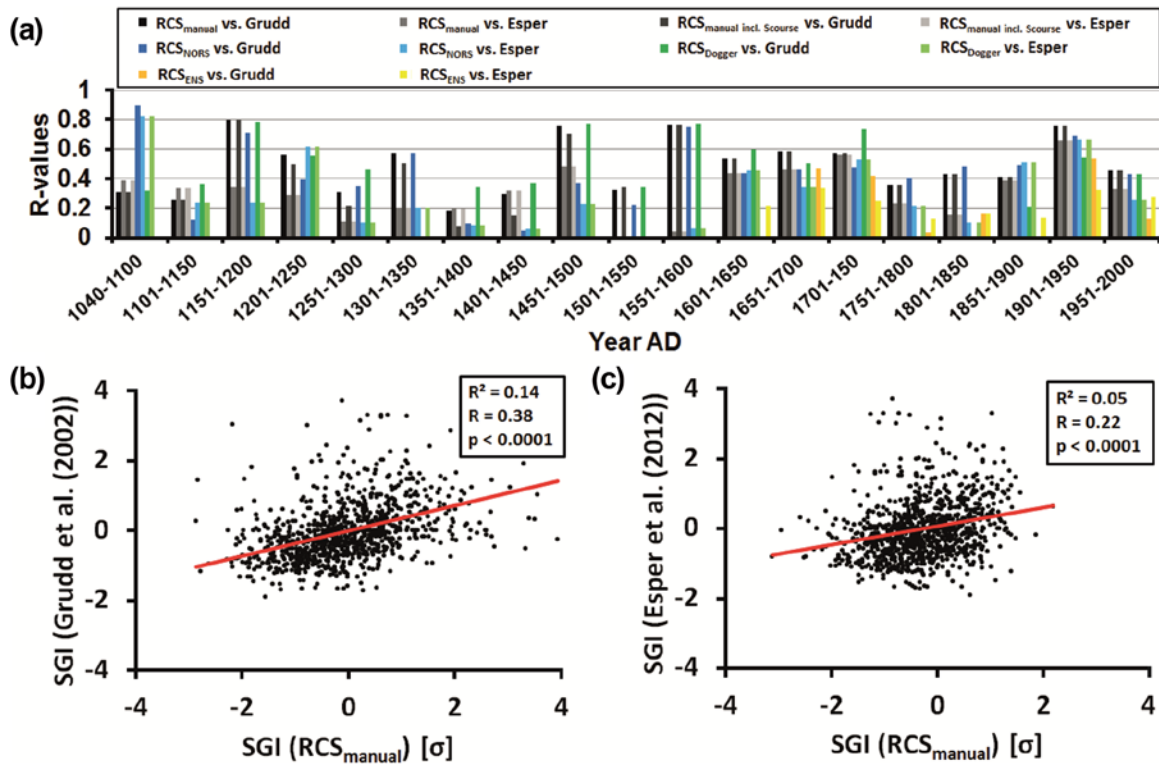


Figure 4. Comparison of growth signals between different localities of the present study. (a) Color-coded sample depths. Note, that the color-coding is maintained in the whole figure. (b–d) Regression analyses between the local RCS_{manual} GI time-series.

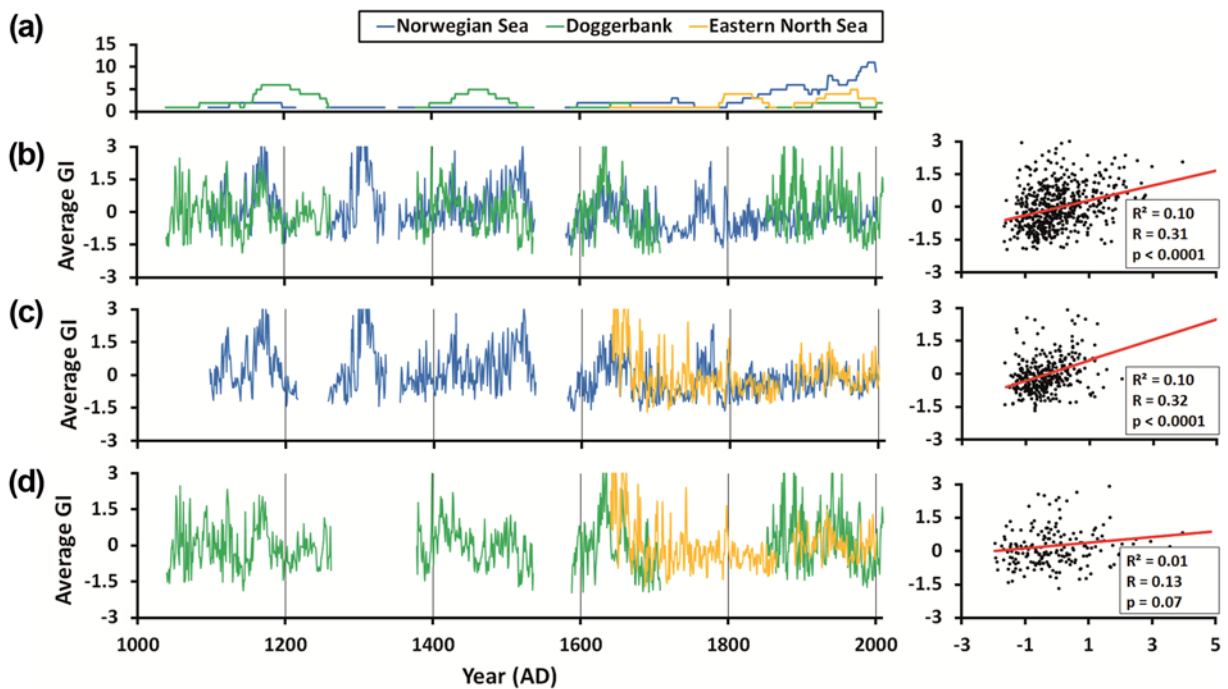


Figure 5. Regression analysis between the different shell chronology versions and the Scandinavian tree-ring reference chronologies. R values in 50-year segments (a) scatter plots between the whole RCS_{manual} chronology and both tree-ring time-series (b) Grudd et al. (2002) and (c) Esper et al. (2012).

occurred in the NE_{ARSTAN} time-series, but the 5% significance level was only reached between around 1400 and 1650, that is, the coldest interval of the LIA, including the Spörer and Maunder sunspot minima (Figure 8c). According to the NE_{ARSTAN} chronology, a transient shift occurred from higher frequency modes during the Medieval Warmth to low-frequency modes during the LIA, and back toward higher frequency oscillations during the

Modern Warmth (Figure 8). In turn, these were lying mostly outside of the significance level.

Furthermore, we observed intermittently strong and highly significant (5% significance level) spectral density at periods of less than 80 years throughout the last millennium (Figure 8); 28–36 and 50–80 year bands dominated periods of sunspot maxima, for example, during the Medieval Warmth and between $c.$

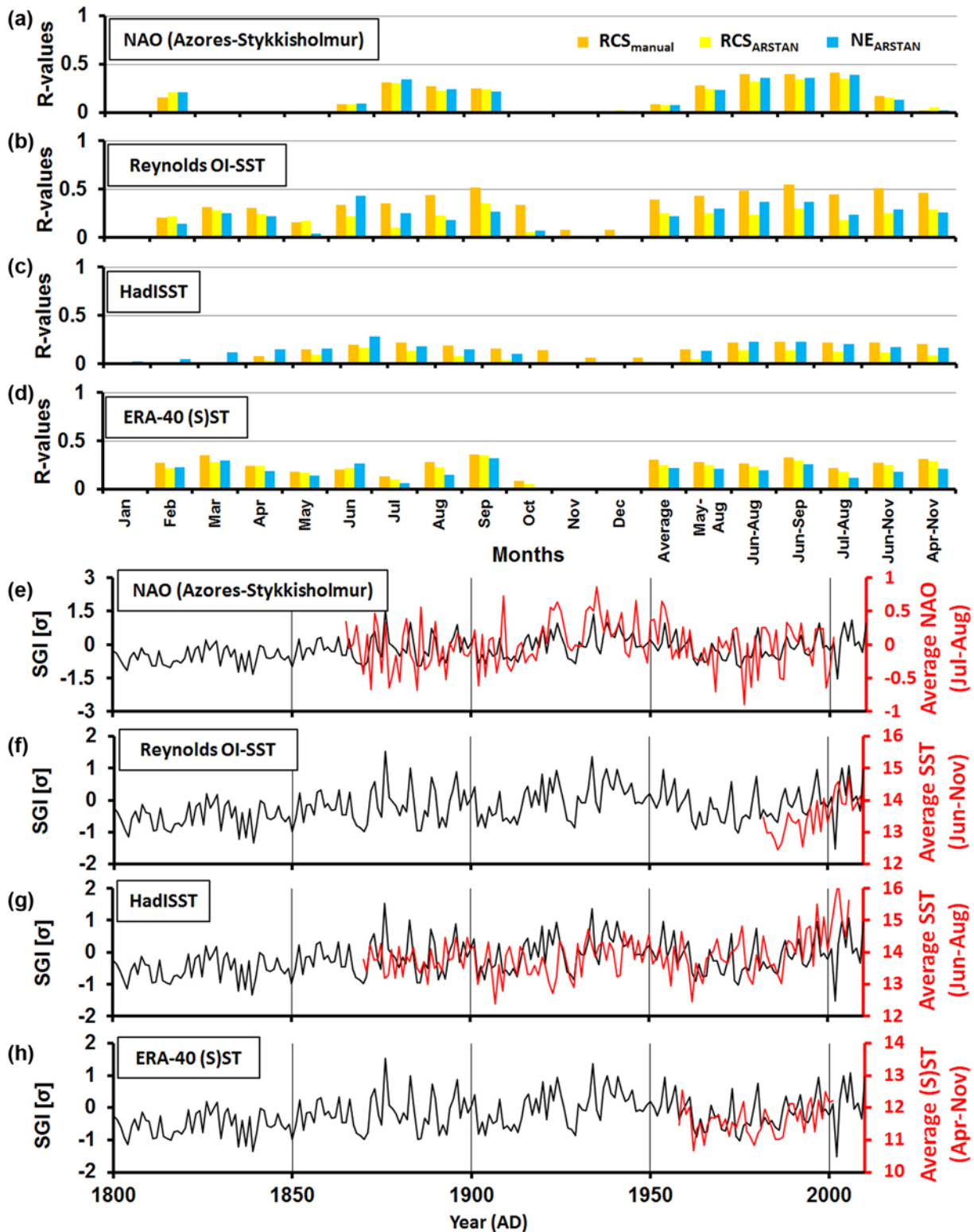


Figure 6. Calibration between the different versions of the North Sea bivalve sclerochronology with instrumental datasets. (a–d) Monthly and seasonally calculated R values with (a) North Atlantic Oscillation (NAO) Index (1900–2001), (b) Reynolds OI-SST (1982–2001), (c) HadISST (1900–2001), and (d) ERA-40 (S)ST (1958–2001). Except for NAO, instrumental datasets are spatially averaged over 50°N to 62°N and –2°E to –10°E. (e–h) Curve plots of RCS_{manual} with seasonally averaged instrumental records with the datasets of (a)–(d).

1550 and 1670, whereas the strong and highly significant shorter wavelengths of 3–8 and 12–16 years were observed during the Spörer and Maunder Minima. In case of the Wolf Minimum, we observed higher frequencies directly before the period of reduced sunspot numbers (NE_{ARSTAN}). Yet, statistically significant higher frequency modes (3–8, 12–16 year cycles) were also found during warm phases (e.g. 1100–1200, 1740–1775, and since 1880).

Correlation with instrumental data

Annual shell growth was positively correlated with SST and zonal wind stress in the North Sea realm (Figure 6). Additionally, a positive correlation of shell growth and the NAO index was observed. Overall strongest correlations were found for shell growth and SST during April and November, and for SSP (sea surface pressure) and zonal wind stress between February and

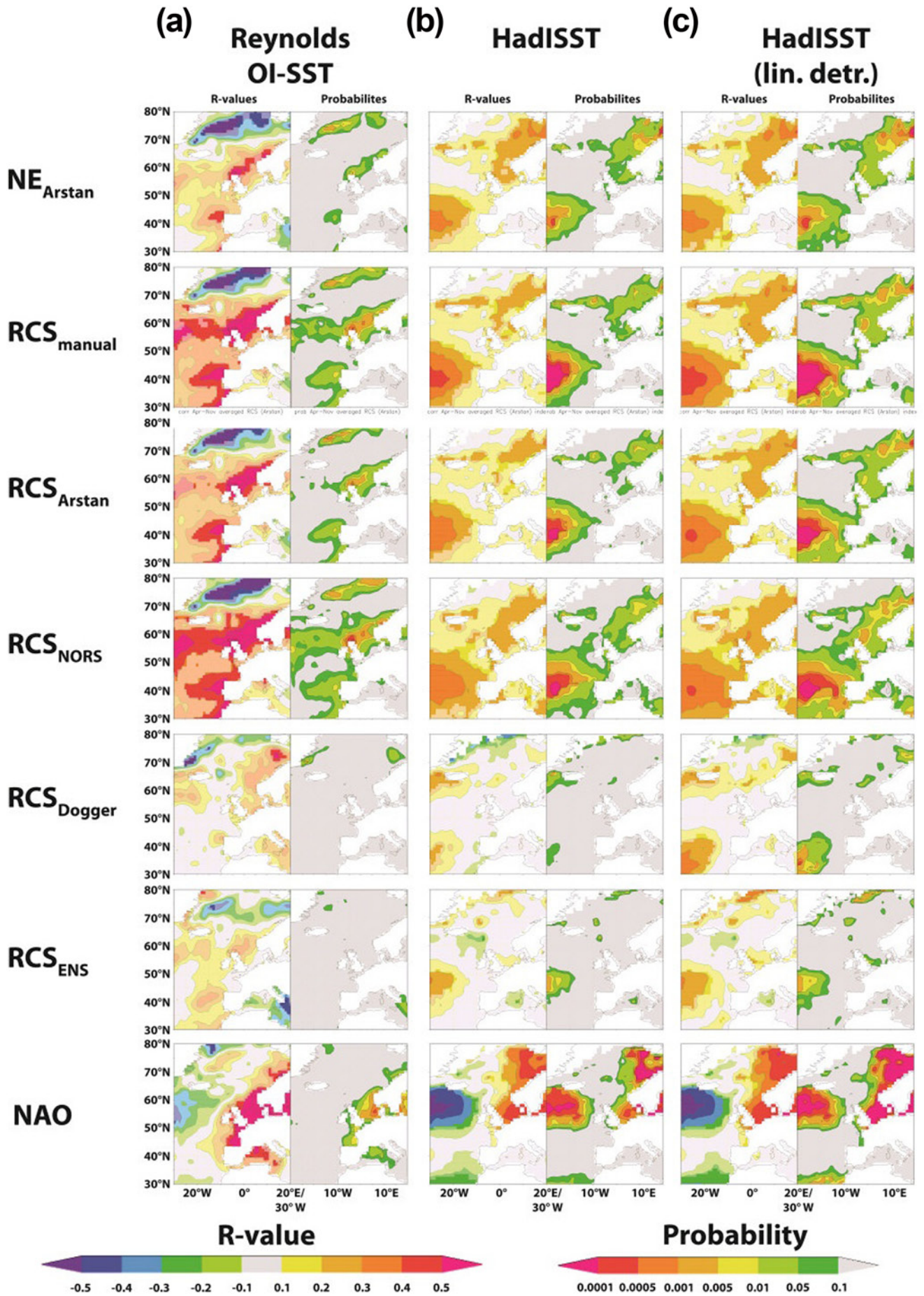


Figure 7. (Continued)

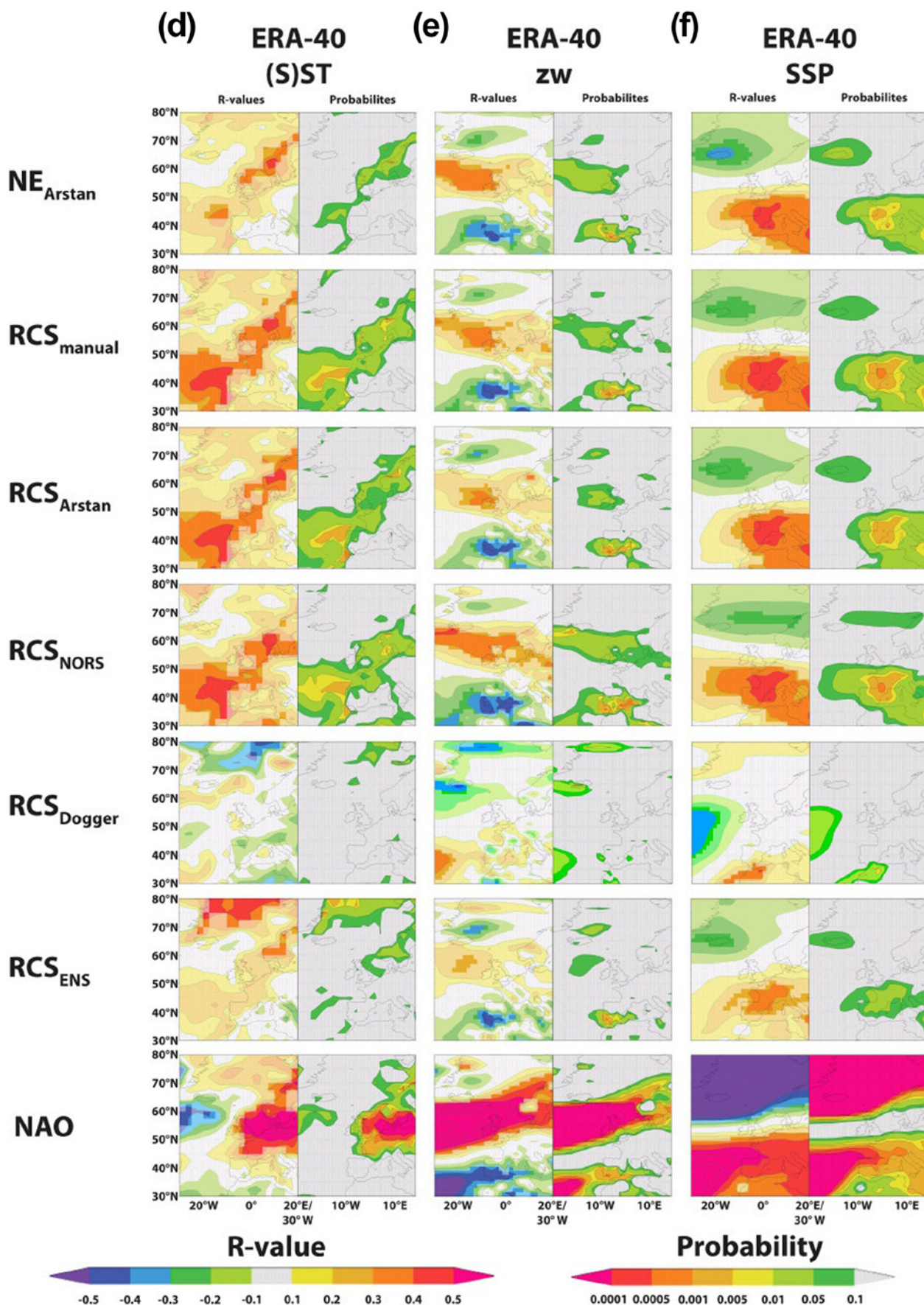


Figure 7. Spatial correlation maps. The three variants of the *Arctica islandica* chronologies (for sample depths >3 shells), the three local time-series of Norwegian Sea (NORS), Doggerbank (Dogger), and Eastern North Sea (ENS) as well as the North Atlantic Oscillation (NAO) index were compared with different (sea) surface temperature (SST) products, zonal wind stress and sea surface pressure (SSP). Increment-temperature comparisons were computed for the April–November average, that is, the main growing season of the bivalves. Regression intervals for sea surface pressure, zonal wind stress, and the NAO time-series are set from February to September. (a) Reynolds OI-SST: 1982–2001; (b) HadISST: 1900–2001; (c) a version using linear detrending of both the HadISST and the shell time-series; (d and e) ERA datasets (temperature, zonal wind stress, sea surface pressure): 1958–2001. Each comparison includes R values (left) and p values (right). Data points with probabilities above 10% in R value maps are drawn in pale colors.

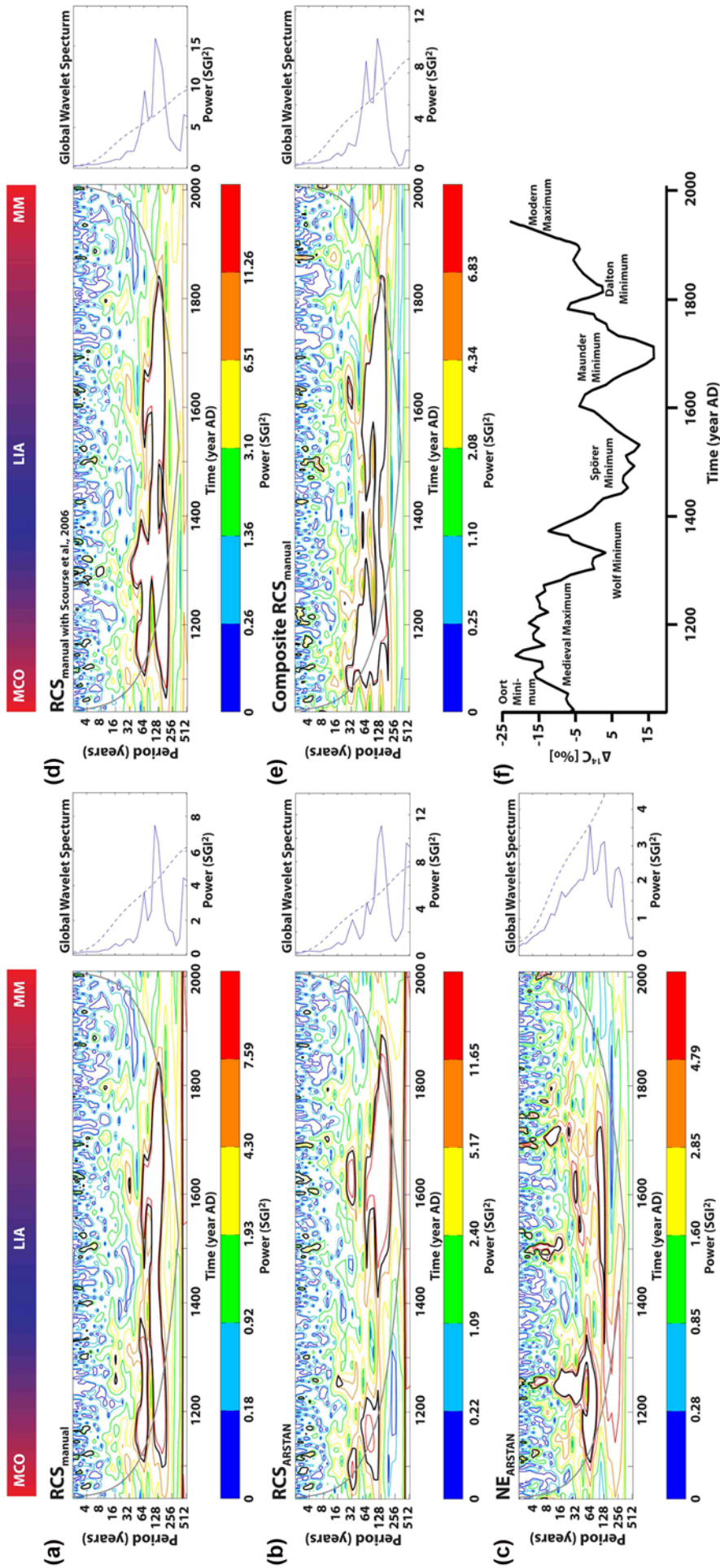


Figure 8. Wavelet transforms (wavenumber 6, Morlet wavelet) and global wavelet spectra of four variants of the Arctic islandica North Sea chronology as shown in Figure 3e–g, k and m. Temporal gaps in the chronology were filled with data from the Scandinavian dendrochronologies to enable calculation of continuous wavelet spectrum. (a) RCS_{manual}, (b) RCS_{ARSTAN}, (c) NE_{ARSTAN}, (d) RCS_{manual} filled with Scourse et al. (2006), and (e) Composite RCS_{manual}. Wavelet transforms provide information on the temporal evolution of signals. The power has been scaled by the global wavelet spectrum (at right). The contour levels are subdivided by the 90%, 80%, 65%, 50%, and 25% percentiles. Black contour is the 5% significance level, using a red-noise background spectrum. The cone of influence, where zero padding has reduced the variance, is illustrated by a gray line. Diagrams produced with MATLAB R2012b and the lon wavelet script, online available at <http://ion.researchsystems.com/>. Note temporal changes of quasi-decadal and multi-decadal variability and their association with cold and warm phases and the sunspot number inversely reflected in the $\Delta^{14}\text{C}$ record (f). RCS: regional curve standardization; MCO: Medieval Climate Anomaly; LIA: Little Ice Age; MW: Modern Warmth.

September. Spatial correlation coefficients were highest (>0.6) for RCS_{manual} and Reynolds OI-SST during 1982–2001 (Figures 6 and 7). Spatial regression analyses for longer time intervals (other surface temperature products and zonal wind stress) returned R values above 0.3–0.4 (Figure 7b–e). In case of HadISST, secondary linear detrending (=elimination of diverging linear trends) applied to the bivalve chronology and the instrumental time-series increased the agreement between the two chronologies. Spatial correlation patterns of the NAO were remarkably similar to that of shell growth and surface temperature, zonal wind stress, or sea surface pressure (Figure 7). According to the spatial regression approach, the similarities between the chronologies and environmental time-series were regionally specific. Furthermore, the local time-series (RCS_{NORS} , RCS_{Dogger} , RCS_{ENS}) exhibited generally lower R values with the instrumental datasets than the multi-regional chronology.

Discussion

Since bivalve shell formation is governed by environmental conditions, growth curves of specimens with overlapping life spans can be cross-dated. Based on this method, it was possible to combine annual increment width chronologies of live-collected and fossil *A. islandica* specimens from different localities of the North Sea into chronologies covering nearly one millennium. Our time-series is the longest ever reported, absolutely dated bivalve sclerochronology from this region, offering a detailed insight into the climate history of the North Sea since 1040 and further contributing to the bivalve shell-based sclerochronological network (Butler et al., 2009a). Existing *A. islandica* chronologies from the North Sea covered the most recent 100–245 years (Butler et al., 2009a: 1870–1979; Epplé et al., 2006: 1840–2003; Schöne et al., 2003: 1757–2001; Witbaard et al., 1997: 1892–1991). Longer stacked records of *A. islandica* from the NE Atlantic came from the Skaggerak, Kattegat, and Øresund (Dunca et al., 2009: c. 200 years), the Irish Sea (Butler et al., 2009b: 489 years), and Iceland (Butler et al., 2013: 1363 years; Lohmann and Schöne, 2013: 508 years).

Spatial coherence of climate signals: multi-regional chronology

An important difference to existing *A. islandica* chronologies (e.g. Butler et al., 2009a, 2009b; Witbaard et al., 1997) is the larger spatial coverage of the stacked record presented here. On the expense of synchronicity between individual time-series, our multi-regional chronologies largely reflected supra-regional climate signals. The specimens that were used to construct the multi-regional chronologies came from various different localities in the entire North Sea (Figure 1; Table 1) and were most likely exposed to very different local climate regimes. As a consequence, the agreement between increment width chronologies of contemporaneous specimens was lower than in many previous *A. islandica* studies. EPS values barely exceeded the 0.85 threshold even at times when six to eight specimens were available (Figure 3). For similar and lower sample depths, for example, Butler et al. (2013) reported EPS values greater than 0.95, indicating a large degree of running similarity. However, the shells used by Butler et al. (2009a, 2009b, 2012) were obtained from a much smaller region and belonged to the same population of bivalves. In fact, it is well known that the running similarity is largest among specimens of the same population, whereas the synchronicity decreases with increasing geographic distance between the populations (Marchitto et al., 2000). For example, in the northern North Sea (Fladen Ground), Butler et al. (2009a) found strongly coherent shell growth over distances of c. 80 km. In the same region, Witbaard et al. (1997) found common signals including variations at

small regional scales as well. By sub-dividing our dataset into local chronologies, it became evident that the localities shared common environmental signals. Even though shell chronologies reached high internal correlations at the local scale, the multi-regional chronologies exhibited only low EPS values indicating the preservation of local signals.

By combining time-series from many different localities, it was possible to capture over-regional climate signals. According to Dunca et al. (2009), low-frequency components of stacked *A. islandica* chronologies from the Skaggerak and Øresund (c. 300 km distance) were largely in phase. Likewise, spatial coherence of the chronologies presented here was also based on low-frequency signals which prevailed in the entire North Sea realm and especially at greater water depths exerted a strong control on *A. islandica* living at different localities in the North Sea and also influenced the growth of trees on land. However, this does not mean that the series were incongruent in the high-frequency domain (Figures 4 and 5).

Spatial coherence based on lower and higher frequencies can be used for cross-dating purposes (Fritts, 1976). This demonstrably works even across kingdom boundaries, that is, bivalve shells and trees (Black et al., 2009; Schöne and Fiebig, 2009). For example, Black et al. (2009) successfully cross-dated increment width chronologies of trees and geoduck shells, *Panopea abrupta*, in the NE Pacific to reconstruct SST. Schöne and Fiebig (2009) demonstrated the possibility to temporally align individual fossil shells of *A. islandica* through cross-dating with the Torneträsk dendrochronology (Esper et al., 2012; Grudd et al., 2002). This cross-dating concept was adopted in this study and used to assign precise calendar years to two $^{14}\text{C}_{\text{AMS}}$ dated floating chronologies (Figure 5).

Additionally, we tested two different procedures of constructing chronologies. Besides the conventional method of averaging all individual time-series, the composite chronology was generated with an arithmetic mean of the four local chronologies (RCS_{NORS} , RCS_{Dogger} , RCS_{ENS} , Scourse et al., 2006). This approach has the advantage of weighing each locality equally. A major disadvantage is a significantly higher variance resulting from stronger influences of individual signals during time intervals of lower sample depths.

Since only two ('F1' and 'F5') of the Butler et al. (2009) time-series fit to the Witbaard et al. (1997) chronology ($R_{1900-1979} = 0.1-0.11$), it was difficult to compare the chronologies presented in this study with the shell growth dynamics at Fladen Ground. The Norwegian Sea sub-chronology compared best with the Fladen Ground chronologies and displayed the highest statistical agreement ($R_{1900-1979} = 0.09-0.16$). Furthermore, we observed a significant decrease in the correlation between the chronology of Witbaard et al. (1997) and our RCS_{NORS} prior to 1975. A 1-year lag of the chronology by Witbaard et al. (1997) increased the correlation significantly ($R_{1925-2000} = 0.19$).

Climate oscillations

As reported in previous studies (Butler et al., 2012; Helama et al., 2007; Lohmann and Schöne, 2013; Schöne et al., 2003; Wanmaker et al., 2009), periodic changes in shell growth of *A. islandica* reflected well-known atmospheric and oceanic climate oscillations. For example, the high-frequency components in the 3- to 8-year and 12- to 16-year band seem to be most likely associated with the NAO and coupled ocean-atmosphere interactions in the subpolar North Atlantic (Deser and Blackmon, 1993; Dima and Lohmann, 2004; Park and Latif, 2005), respectively. It should be noted that high-frequency modes can be the product of random autoregressive memory effects (Wunsch, 1999). However, the spectral signal strength of the transitions exceeded the red-noise null hypothesis taking into account autoregressive processes.

The observed multi-decadal oscillations in shell growth (28–36, 50–80, 120–240 years) compare well with fluctuations in temperature and circulation patterns associated with AMOC and ultimately reflect temporal changes of the Atlantic water inflow into the North Sea (Witbaard et al., 1997, 2003). In order to interpret low-frequency signals, the so-called segment length curse has to be taken into consideration (Cook et al., 1995). The curse describes a fundamental problem of reduced low-frequency responses in time-series analysis that is coupled to detrending and standardization techniques. Here, this effect becomes evident by comparing the individually detrended NE_{Arstan} with the RCS chronologies. Whereas NE_{Arstan} is eliminating large portions of the low-frequencies, they are much better preserved in the RCS chronologies. Periodicities that exceed the average life span of specimens used in the composite chronology should be interpreted with caution.

Surprisingly, the strength and statistical significance of the different quasi-decadal and multi-decadal climate modes during the last millennium seem to be associated with the sunspot cycles as well as warm and cold periods (Figure 8). Atmospheric and coupled ocean–atmosphere signals (quasi-decadal components) were particularly pronounced during the sunspot minima (Figure 5). For example, the 3- to 8-year and 12- to 16-year periods were stronger at around 1500, that is, close to the beginning of the LIA (Lamb, 1965). Similar findings have been reported from other *A. islandica* composite chronologies and other climate proxy archives (Butler et al., 2013; Christiansen, 1998; Lohmann and Schöne, 2013). According to historical documents (Ogilvie and Jónsson, 2001), wind stress and the inter-annual climate variability were much higher during this climatic regime shift (Trouet et al., 2012).

Warm intervals such as the Medieval Maximum, however, were dominated by signals in the range of 28–36 and 50–80 years, that is, the periodicity of AMOC. As a consequence, the northward heat transport became stronger and led to warmer conditions in the NE Atlantic realm (Lund et al., 2006; Wanamaker et al., 2012). Prolonged time intervals of stable climate conditions during the culmination phase of the LIA may be explained by the predominance of low-frequency variations (120–240 years) in oceanic heat transport.

In summary, stronger inter-annual to quasi-decadal variability was associated with a strong atmospheric forcing and outstanding sunspot minima. Occasionally, phases of increased climatic instability fell together with periods of high sunspots numbers. More stable climatic conditions (warm or cold), however, were observed in conjunction with a predominance of multi-decadal variability, maybe related to the AMOC. Whether a causal link exists between the sunspot number and the NAO as suggested by other authors (Van Loon et al., 2012) should be critically assessed in future studies and by including other annually resolved climate proxy records from the NE Atlantic realm.

Environmental controls on shell growth

According to spatial regression analyses (Figure 4), shells of *A. islandica* grew faster when surface waters were warmer and westerlies were stronger (positive NAO) between April and November. This correlation may be associated to the greater water depth in which the bivalves lived, where more constant conditions prevailed throughout the growing season. However, no direct link can have existed between the growth of bivalves that lived below the thermocline and environmental conditions prevailing at sea surface between spring and fall. Only when the thermocline disrupts in winter, warm surface waters are mixed downward and reach the sites where the bivalve lives (OSPAR Commission, 2000). It is more likely that faster growth of the bivalves is indirectly linked to surface water conditions. Higher productivity

rates in warm surface waters were followed by higher levels of organic debris reaching the sea floor that nurtured the bivalves.

Conversely, increased westerlies associated with the NAO likely increased the speed of currents, which in turn can have resulted in increased amounts of re-suspended organic particles near the bottom of the sea, and hence increased food levels. A positive relationship between benthic productivity and decadal climate modes has also been identified in many previous studies (Kröncke et al., 2001; Witbaard et al., 1997). Decadal cycles of temperature and the availability and quality of food may also have influenced the reproductive success of *A. islandica* (recruitment cycles) and may serve as an explanation for the observed distribution of fossils through time (Figure 3). Apparently, maximum and minimum abundances of shells alternated periodically every c. 240 years (Figure 3). However, additional data are required to verify this hypothesis, for example, a statistically robust map showing the age distributions of *A. islandica* in various parts of the North Sea.

Temperature fluctuations may also explain the observed changes in average longevity of *A. islandica* during the last millennium. Although this species is well adapted to low temperature conditions and demonstrably grows during winter even at much higher latitudes (Schöne, 2008), colder water may result in reduced growth rates. Shells growing at lower rates during early ontogeny will likely reach the predation window and maturity at a later age than specimens growing quickly during youth. Therefore, slower growth rates can increase the life expectancy. Notably, the oldest ever reported specimens of *A. islandica*, for example, a 374-year-old ‘Methuseloh’ from E Iceland (Schöne et al., 2005b) and a 507-year-old specimen from North Iceland (Butler et al., 2013) were born during the Spörer Minimum. Decreased average longevity during the 20th century, however, is more likely the result of overfishing in the North Sea (e.g. Coll et al., 2008).

Summary and conclusion

We presented the first multiregional *A. islandica* chronologies which cover nearly the entire 2nd millennium AD and contain information on over-regional climate conditions (SST, ocean productivity, wind stress), which were modulated by the atmosphere and ocean. Cycles of shell growth were closely associated with the NAO (3–8 years), ocean-internal cycles of the NE Atlantic (12–16 years) and the AMOC (28–36, 50–80, 120–240 years). The higher frequency components, maybe indicative of increased climate instability, occurred predominantly during the major sunspot minima and during particularly warm intervals, whereas the low-frequency, oceanic components prevailed during more stable climate conditions, that is, extended warm or cold periods. The link and potential mechanisms between the activity of the sun and dominance of certain climate modes need to be addressed in upcoming studies.

In order to identify and quantify long-term climate trends through the last millennium, future studies should focus on the geochemical proxy record which is not subject to the ‘segment length curse’ (Cook et al., 1995). As demonstrated here, variations in shell growth can provide important information on decadal climate variability, but the reconstruction of longer term climatic oscillations and trends is limited by the length of the individual chronologies used to build the chronology.

Furthermore, a cross-calibration with other *A. islandica* composite chronologies from the northern North Atlantic (Butler et al., 2012; Lohmann and Schöne, 2013; Scourse et al., 2006; Wanamaker et al., 2008; Witbaard et al., 1997) as well as other high-resolution paleoclimate archives such as tree rings, speleothem records, varved sediments, and so on (Briffa et al., 1992; Esper et al., 2002; Fohlmeister et al., 2012; Grudd et al., 2002;

Scholz et al., 2012; Sirocko et al., 2012; Vollweiler et al., 2006) can help to draw a more detailed picture of the climatic past of Europe. Such information is relevant to test, verify, and improve predictions of possible future climates in this region. The new EU-funded international collaboration Annually Resolved Archives of Marine Climate Change (ARAMACC) will certainly contribute to a better understanding of past European marine climate conditions.

Acknowledgements

Shells used in this study were kindly provided by Wolfgang Dreyer (University of Kiel, Germany), Ingrid Kröncke (Senckenberg am Meer, Wilhelmshaven, Germany), Ronald Janssen and Michael Tuerkay (Senckenberg Research Institute and Natural History Museum, Frankfurt/Main, Germany), Heye Rumohr (Geomar/Helmholtz Centre for Ocean Research, Kiel, Germany), and Annemiek Vink (Bundesanstalt für Geowissenschaften und Rohstoffe, Hannover, Germany). We are grateful to Paul Butler, James Scourse (School of Ocean Sciences, Bangor University), and Rob Witbaard (NIOZ, Royal Netherlands Institute for Sea Research) for providing bivalve sclerochronologies from Fladen Ground. We are greatly indebted to Michael Maus for his help during laboratory work. Furthermore, we want to express our thanks to Paul Butler and an anonymous reviewer for their helpful and constructive suggestions.

Funding

This study has been made possible by a PhD scholarship of the Earth System Research Center Geocycles (to HAH) and a grant by the German Research Foundation (DFG) (to BRS: SCHO793/10).

References

- Black BA (2009) Climate-driven synchrony across tree, bivalve, and rockfish growth-increment chronologies of the northeast Pacific. *Marine Ecology Progress Series* 378: 37–46.
- Black BA, Copenheaver CA, Stuckey MJ et al. (2009) Multi-proxy reconstructions of northeastern Pacific sea surface temperature data from trees and Pacific geoduck. *Palaeogeography, Palaeoclimatology, Palaeoecology* 278: 40–47.
- Briffa K and Jones P (1990) Basic chronology statistics and assessment. In: Cook E and Kairiukstis L (eds) *Methods of Dendrochronology: Applications in the Environmental Sciences*. Dordrecht: Kluwer Academic, pp. 137–152.
- Briffa KR, Jones PD, Bartholin TS et al. (1992) Fennoscandian summers from AD 500: Temperature changes on short and long timescales. *Climate Dynamics* 7: 111–119.
- Büntgen U, Tegel W, Nicolussi K et al. (2012) 2500 years of European climate variability and human susceptibility. *Science* 331: 578–582.
- Butler PG, Richardson CA, Scourse JD et al. (2009a) Accurate increment identification and the spatial extent of the common signal in five *Arctica islandica* chronologies from the Fladen Ground, northern North Sea. *Paleoceanography* 24: PA2210. DOI: 10.1029/2008PA001715.
- Butler PG, Richardson CA, Scourse JD et al. (2010) Marine climate in the Irish Sea: Analysis of a 489-year marine master chronology derived from growth increments in the shell of the clam *Arctica islandica*. *Quaternary Science Reviews* 29: 1614–1632.
- Butler PG, Scourse JD, Richardson CA et al. (2009b) Continuous marine radiocarbon reservoir calibration and the 13C Suess effect in the Irish Sea: Results from the first multi-centennial shell-based marine master chronology. *Earth and Planetary Science* 279: 230–241.
- Butler PG, Wanamaker AD, Scourse JD et al. (2013) Variability of marine climate on the North Icelandic Shelf in a 1357-year proxy archive based on growth increments in the bivalve *Arctica islandica*. *Palaeogeography, Palaeoclimatology, Palaeoecology* 373: 141–151.
- Coll M, Libralato S, Tudela S et al. (2008) Ecosystem overfishing in the ocean. *PLoS One* 3: e3881. DOI: 10.1371/journal.pone.0003881.
- Cook ER and Peters K (1997) Calculating unbiased tree-ring indices for the study of climatic and environmental change. *The Holocene* 7: 361–370.
- Cook ER, Briffa KR, Meko DM et al. (1995) The ‘segment length curse’ in long tree-ring chronology development for paleoclimate studies. *The Holocene* 5: 229–237.
- Cunningham LK, Austin WEN, Knudson KL et al. (2013) Reconstructions of surface ocean conditions from the northeast Atlantic and Nordic seas during the last millennium. *The Holocene* 23: 921–935.
- Delworth TL and Mann ME (2000) Observed and simulated multidecadal variability in the Northern Hemisphere. *Climate Dynamics* 16: 661–676.
- Deser C and Blackmon M (1993) Surface climate variations over the North Atlantic Ocean during winter: 1900–1989. *Journal of Climate* 6: 1743–1753.
- Dima M and Lohmann G (2004) Fundamental and derived modes of climate variability. Application to biennial and interannual timescale. *Tellus* 56: 229–249.
- Dunca E, Mutvei H, Göransson P et al. (2009) Using ocean quahog (*Arctica islandica*) shells to reconstruct paleoenvironment in Öresund, Kattegat and Skagerrak, Sweden. *International Journal of Earth Science* 98: 3–17.
- Epplé VM, Brey T, Witbaard R et al. (2006) Sclerochronological records of *Arctica islandica* from the inner German Bight. *The Holocene* 16: 763–769.
- Esper J, Cook ER and Schweingruber FH (2002) Low-frequency signals in long tree-ring chronologies for reconstructing past temperature variability. *Science* 295: 2250–2253.
- Esper J, Frank DC, Timonen M et al. (2012) Orbital forcing of tree-ring data. *Nature Climate Change* 2: 862–866.
- Fohlmeister J, Schröder-Ritzrau A, Scholz D et al. (2012) Bunker Cave stalagmites: An archive for central European Holocene climate variability. *Climate of the Past* 8: 1751–1764.
- Fritts HC (1976) *Tree Rings and Climate*. London: Academic Press. 567 pp.
- Greatbatch RJ (2000) The North Atlantic Oscillation. *Stochastic Environmental Research and Risk Assessment* 14: 213–242.
- Grissino-Mayer HD (2001) Evaluating crossdating accuracy: A manual and tutorial for the computer program COFECHA. *Tree-Ring Research* 57: 205–221.
- Grudd H, Briffa KR, Karlén W et al. (2002) A 7400-year tree-ring chronology in northern Swedish Lapland: Natural climate variability expressed on annual to millennial timescales. *The Holocene* 12: 657–665.
- Harkness DD (1983) The extent of natural ¹⁴C deficiency in the coastal environment of the United Kingdom. *PACT* 8: 351–364.
- Helama S, Schöne BR, Kirchhefer AJ et al. (2007) Compound response of marine and terrestrial ecosystems to varying climate: Pre-anthropogenic perspective from bivalve shell growth increments and tree-rings. *Marine Environmental Research* 63: 185–199.
- Hughen KA, Baillie MGL, Bard E et al. (2004) Marine radiocarbon age calibration, 0–26 cal. kyr BP. *Radiocarbon* 46: 1059–1086.

- Hurrell JW (1995) Decadal trends in the North Atlantic Oscillation: Regional temperatures and precipitation. *Science* 269: 676–679.
- IPCC (2007) *Fourth assessment report, climate change 2007: The physical science basis*. Contribution of Working Group I to the Fourth Assessment Report of the Intergovernmental Panel on Climate Change, Report no. AR 4, March. Cambridge: Cambridge University Press.
- Jones PD, Osborn TJ and Briffa KR (2001) The evolution of climate over the last millennium. *Science* 292: 662–667.
- Jones PD, Briffa KR, Osborn TJ et al. (2009) High-resolution palaeoclimatology of the last millennium: A review of current status and future prospects. *The Holocene* 19: 3–49.
- Kröncke I, Zeiss B and Rensing C (2001) Long-term variability in macrofauna species composition off the island of Norderney (East Frisia, Germany) in relation to changes in climatic and environmental conditions. *Senckenbergiana maritima* 31: 65–82.
- Lamb HH (1965) The early medieval warm epoch and its sequel. *Paleogeography, Paleoclimatology, Paleoecology* 1: 13–37.
- Lohmann G and Schöne BR (2013) Climate signatures on decadal to interdecadal time scales as obtained from mollusk shells (*Arctica islandica*) from Iceland. *Paleogeography, Paleoclimatology, Paleoecology* 373: 152–162.
- Lund DC, Lynch-Stieglitz J and Curry WB (2006) Gulf Stream density structure and transport during the past millennium. *Nature* 444: 601–604.
- Marchitto TM, Jones GA, Goodfriend GA et al. (2000) Precise temporal correlation of Holocene mollusk shells using sclerochronology. *Quaternary Research* 53: 236–246.
- Mangerud J and Gulliksen S (1975) Apparent radiocarbon ages of recent marine shells from Norway, Spitsbergen and Arctic Canada. *Quaternary Research* 5: 263–273.
- Needleman SB and Wunsch CD (1970) A general method applicable to the search for similarities in the amino acid sequence of two proteins. *Journal of Molecular Biology* 48: 443–453.
- Ogilvie AEJ and Jónsson T (2001) Little Ice Age research: A perspective from Iceland. *Climatic Change* 48: 9–52.
- OSPAR Commission (2000) *Quality Status Report 2000, Region II – Greater North Sea*. London: OSPAR Commission.
- Park W and Latif M (2005) Ocean dynamics and the nature of air–sea interactions over the North Atlantic. *Journal of Climate* 18: 982–995.
- Rayner NA, Parker DE, Horton EB et al. (2003) Global analyses of sea surface temperature, sea ice, and night marine air temperature since the late nineteenth century. *Journal of Geophysical Research: Atmospheres* 108: D14. DOI: 10.1029/2002JD002670.
- Reynolds RW (1988) A real-time global sea surface temperature analysis. *Journal of Climate* 1: 75–86.
- Reynolds RW and Smith TM (1995) A high resolution global sea surface temperature climatology. *Journal of Climate* 8: 1571–1583.
- Reynolds DJ, Butler PG, Williams SM et al. (2013) A multiproxy reconstruction of Hebridean (NW Scotland) spring sea surface temperatures between AD 1805 and 2010. *Paleogeography, Palaeoclimatology, Palaeoecology* 386: 275–285.
- Scheslinger ME and Ramankutty N (1994) An oscillation in the global climate system of period 65–70 years. *Nature* 367: 723–726.
- Scholz D, Frisia S, Borsato A et al. (2012) Holocene climate variability in north-eastern Italy: Potential influence of the NAO and solar activity recorded by speleothem data. *Climate of the Past* 8: 1367–1383.
- Schöne BR (2008) The curse of physiology – Challenges and opportunities in the interpretation of geochemical data from mollusk shells. *Geo-Marine Letters* 28: 269–285.
- Schöne BR and Fiebig J (2009) Seasonality in the North Sea during the Allerød and Late Medieval Climate Optimum using bivalve sclerochronology. *International Journal of Earth Sciences* 98: 83–98.
- Schöne BR, Dunca E, Fiebig J et al. (2005a) Mutvei's solution: An ideal agent for resolving microgrowth structures of biogenic carbonates. *Palaeogeography, Palaeoclimatology, Palaeoecology* 228: 149–166.
- Schöne BR, Fiebig J, Pfeiffer M et al. (2005b) Climate records from a bivalved Methuselah (*Arctica islandica*, Mollusca; Iceland). *Palaeogeography, Palaeoclimatology, Palaeoecology* 228: 130–148.
- Schöne BR, Oschmann W, Rössler J et al. (2003) North Atlantic Oscillation dynamics recorded in shells of a long-lived bivalve mollusk. *Geology* 31: 1037–1040.
- Schöne BR, Zhang Z, Radermacher P et al. (2011) Sr/Ca and Mg/Ca ratios of ontogenetically old, long-lived bivalve shells (*Arctica islandica*) and their function as paleotemperature proxies. *Palaeogeography, Palaeoclimatology, Palaeoecology* 302: 52–64.
- Schweingruber FH, Eckstein D, Serre-Bachet F et al. (1990) Identification, presentation and interpretation of event years and pointer years in dendrochronology. *Dendrochronologia* 8: 9–38.
- Scourse J, Richardson A, Forsythe G et al. (2006) First cross-matched floating chronology from the marine fossil record: Data from growth lines of the long-lived bivalve mollusc *Arctica islandica*. *The Holocene* 16: 967–974.
- Sirocko F, Dietrich S, Veres D et al. (2012) Multi-proxy dating of Holocene maar lakes and Pleistocene dry maar sediments in the Eifel, Germany. *Quaternary Science Reviews* 62: 56–76.
- Smith TM and Reynolds RW (1998) A high resolution global sea surface temperature climatology for the 1961–90 base period. *Journal of Climate* 11: 3320–3323.
- Smith TF and Waterman MS (1981) Identification of common molecular subsequences. *Journal of Molecular Biology* 147: 195–197.
- Stuiver M, Reimer PJ and Braziunas TF (1998) High-precision radiocarbon age calibration on terrestrial and marine samples. *Radiocarbon* 40: 1127–1151.
- Thompson I, Jones DS and Dreibeilbis D (1980) Annual inter-annual growth banding and life history of the ocean quahog *Arctica islandica* (Mollusca: Bivalvia). *Marine Biology* 57: 25–34.
- Torrence C and Compo GP (1998) A practical guide to wavelet analysis. *Bulletin of the American Meteorological Society* 79: 61–78.
- Trouet V and Van Oldenborgh GJ (2013) Research tools – KNMI Climate Explorer: A web-based tool for high-resolution paleoclimatology. *Tree-Ring Research* 69: 3–13.
- Trouet V, Scourse JD, Raible CC (2012) North Atlantic storminess and Atlantic meridional overturning circulation during the last Millennium: Reconciling contradictory proxy records of NAO variability. *Global and Planetary Change* 84–85: 48–55.
- Turrell WR (1992) New hypotheses concerning the circulation of the northern North Sea and its relation to North Sea fish stock recruitment. *ICES Journal of Marine Science* 49: 107–123.
- Turrell WR, Henderson EW, Slessor G et al. (1992) Seasonal changes in the circulation of the northern North Sea. *Continental Shelf Research* 12: 257–286.
- Uppala SM, Kallberg PW, Simmons AJ et al. (2005) The ERA-40 re-analysis. *Quarterly Journal of the Royal Meteorological Society* 131: 2961–3012.
- Van Loon H and Rogers JC (1978) The seesaw in winter temperatures between Greenland and northern Europe. Part I: General description. *Monthly Weather Review* 106: 296–310.

- Van Loon H, Brown J and Milliff R (2012) Trends in sunspots and North Atlantic sea-level pressure. *Journal of Geophysical Research* 117: D7. DOI: 10.1029/2012JD017502.
- Vollweiler N, Scholz D, Mühlinghaus C et al. (2006) A precisely dated climate record for the last 9 kyr from three high alpine stalagmites, Spannagel Cave, Austria. *Geophysical Research Letters* 33: L20703. DOI: 10.1029/2006GL027662.
- Wanamaker AD, Butler PG, Scourse JD et al. (2012) Surface changes in the North Atlantic meridional overturning circulation during the last millennium. *Nature Communications* 3: 899. DOI: 10.1038/ncomms1901.
- Wanamaker AD, Heinemeier J, Scourse JD et al. (2008) Very long-lived mollusks confirm 17th century AD tephra-based radiocarbon reservoir ages for north Icelandic shelf waters. *Radiocarbon* 50: 399–412.
- Wanamaker AD, Kreuz K, Schöne BR et al. (2009) A late Holocene paleo-productivity record in the western Gulf of Maine, USA, inferred from growth histories of the long-lived ocean quahog (*Arctica islandica*). *International Journal of Earth Sciences* 98: 19–29.
- Wei W and Lohmann G (2012) Simulated Atlantic multidecadal oscillation during the Holocene. *Journal of Climate* 25: 6989–7002.
- Wigley TML, Briffa KR and Jones PD (1984) On the average value of correlated time series, with applications in dendroclimatology and hydrometeorology. *Journal of Climate and Applied Meteorology* 23: 201–213.
- Wilson RJS, Cook E, D'Arrigo R et al. (2010) Reconstructing ENSO: The influence of method, proxy data, climate forcing and teleconnections. *Journal of Quaternary Science* 25: 62–78.
- Witbaard R, Duineveld GCA and de Wilde PAWJ (1997) A long-term growth record derived from *Arctica islandica* (Mollusca, Bivalvia) from the Fladen Ground (northern North Sea). *Journal of the Marine Biological Association of the United Kingdom* 77: 801–816.
- Witbaard R, Jansma E and Sass Klaassen U (2003) Copepods link quahog growth to climate. *Journal of Sea Research* 50: 77–83.
- Woollings T (2010) Dynamical influences on European climate: An uncertain future. *Philosophical Transactions of the Royal Society A: Mathematical, Physical and Engineering Sciences* 368: 3733–3756.
- Wunsch C (1999) The interpretation of short climate records, with comments on North Atlantic and Southern Oscillation. *Bulletin of the American Meteorological Society* 80: 245–255.

Copyright of Holocene is the property of Sage Publications, Ltd. and its content may not be copied or emailed to multiple sites or posted to a listserv without the copyright holder's express written permission. However, users may print, download, or email articles for individual use.